horticulturae

MDPI

Article

Genome-Wide Identification and Expression Analysis of *AMT* Gene Family in Apple (*Malus domestica* Borkh.)

Linlin Huang [1,2,3], Jiazhen Li [1], Bin Zhang [1], Yanyan Hao [1,*] and Fengwang Ma [2,3,*]

[1] College of Horticulture, Shanxi Agricultural University, Taigu, Jinzhong 030801, China; llhuang@sxau.edu.cn (L.H.); s20202181@stu.sxau.edu.cn (J.L.); jztgzhangbin@sxau.edu.cn (B.Z.)
[2] State Key Laboratory of Crop Stress Biology for Arid Areas, College of Horticulture, Northwest A&F University, Yangling, Xianyang 712100, China
[3] Shaanxi Key Laboratory of Apple, College of Horticulture, Northwest A&F University, Yangling, Xianyang 712100, China
* Correspondence: haoyy@sxau.edu.cn (Y.H.); fwm64@nwsuaf.edu.cn (F.M.)

Abstract: Ammonium is one of the prevalent nitrogen sources for growth and development of higher plants. Ammonium acquisition from soil is facilitated by ammonium transporters (AMTs), which are plasma membrane proteins that exclusively transport ammonium/ammonia. However, the functional characteristics and molecular mechanisms of *AMTs* in apple remain unclear. In this work, 15 putative *AMT* genes were identified and classified into four clusters (AMT1–AMT4) in apple. According to expression analysis, these *AMT*s had varying expressions in roots, leaves, stems, flowers and fruits. Some of them were strongly affected by diurnal cycles. *AMT* genes showed multiple transcript patterns to N regimes and were quite responsive to osmotic stress. In addition, phosphorylation analysis revealed that there were some conserved phosphorylation residues within the C-terminal of AMT proteins. Furthermore, detailed research was conducted on *AMT1;2* functioning by heterologous expression in yeast. The present study is expected to provide basic bioinformatic information and expression profiles for the apple *AMT* family and to lay a basis for exploring the functional roles and regulation mechanisms of *AMTs* in apple.

Keywords: ammonium transporter; apple; expression analysis; osmotic stress

Citation: Huang, L.; Li, J.; Zhang, B.; Hao, Y.; Ma, F. Genome-Wide Identification and Expression Analysis of *AMT* Gene Family in Apple (*Malus domestica* Borkh.). *Horticulturae* **2022**, *8*, 457. https://doi.org/10.3390/horticulturae8050457

Academic Editor: Dilip Panthee

Received: 13 April 2022
Accepted: 15 May 2022
Published: 19 May 2022

1. Introduction

Nitrogen (N) is one of the most important nutrients that contribute to plant growth and fruit quality [1–3]. Inorganic N in most higher plants is mainly sourced from ammonium and nitrate. In the case of N deficiency in plants, ammonium is the preferential form because less energy is required by ammonium assimilation than nitrate assimilation [4]. However, excessive ammonium absorption by plants can be toxic as indicated by inhibitory growth [5]. Therefore, particular attention has been paid to the ammonium uptake system in plants.

Ammonium acquisition in plants is controlled by ammonium transporters (AMTs), which have been recognized in diverse plant species [6–8]. Previous studies have demonstrated that plant AMTs are distributed in the plasma membrane and can constitute homo- or hetero-trimers, enabling passing of NH_4^+ or NH_3 through the pore [9]. It is suggested that plant AMTs may function as a NH_4^+ uniporter, NH_4^+/H^+ symporter or NH_3/H^+ co-transporter. Plant AMTs can be normally divided into the following two subfamilies: AMT1 and AMT2; members of the former represent the best characterized cases. In *Arabidopsis*, *AtAMT1;1/1;3/1;5* contributed additively to 70–80% of the high-affinity ammonium uptake ability in roots [7,10]. Knockout of *OsAMT1;1/1;2/1;3* resulted in a reduction of 90–95% in ammonium uptake and a substantial decrement in the growth and yield [11]. There is evidence denoting that the highly conserved trans-activation domains at the C-termini are determinant of the functionality of plant AMT1s. The phosphorylation of T460 in

AtAMT1;1 led to loss of NH_4^+ uptake activity in response to increasing exogenous NH_4^+ supply [12,13], providing a novel regulatory mechanism that the NH_4^+ transport of AMTs can be rapidly shut off under high NH_4^+ supply.

This manifested that ammonium nutrition functions by mitigating the adverse effects of various abiotic stress, e.g., drought stress [14,15] and salinity stress [16,17], so the AMTs may be active in plant tolerance to abiotic stress. As reported in previous studies, transcript abundance of some *AMTs* increased greatly in roots of *Malus hupehensis* and *Populus simonii* seedlings under osmotic stress [18,19]. In the early root growth stage, salt tolerance was prominently improved by overexpression of *PutAMT1;1* in *Arabidopsis* [20]. Previous research also demonstrated that *AMTs* exhibited species-specific regulatory features in the case of different N regimes in plants. For instance, transcript abundance of *AtAMT1;1* increased while *AtAMT1;2* was not significantly induced by N deprivation in roots [21]. *ZmAMT1;1a* and *ZmAMT1;3* displayed dropped transcript levels during N starvation periods [22]. Taken together, plant *AMT*s in different species exhibit multiple expression patterns in response to various environmental factors, and homologous *AMTs* from species subject to added applied research should be characterized.

In this work, 15 putative *AMT* family members were characterized from the apple (*Malus domestica* Borkh.) genome, and their phylogeny, gene structure, conserved domain and genome location were analyzed. Additionally, cis-elements and phosphorylation of *AMT* family members were also canvassed. Furthermore, the transcription profiles of *AMTs* in various tissues and diurnal rhythms were investigated, and the regulatory response of *AMTs* to different N regimes and osmotic stress was explored. In addition, the function of *AMT1;2* was further studied by yeast complementation assay. Our findings provide basic bioinformatic information and expression profiles for the apple *AMT* family and may present a comprehensive basis for further studies on the ammonium nutrition of fruit trees.

2. Materials and Methods

2.1. Identification of AMT Gene Family Members in Apple

In accordance with previous reports, AMT proteins in *Arabidopsis thaliana* and *Populus trichocarpa* were used as queries against the apple genome database (http://genomics.research.iasma.it/, accessed on 23 June 2021). Following removal of overlapping sequences, loading of *M. domestica* genome annotations from that database was completed. Thereafter, submitting of protein sequences to Pfam (http://pfam.sanger.ac.uk/, accessed on 24 June 2021) and SMART (http://smart.emblheidelberg.de/, accessed on 24 June 2021) was accomplished to confirm the current existence and wholeness of the ammonium domain. ExPASy (https://web.expasy.org/compute_pi/, accessed on 24 June 2021) was utilized for prediction of the molecular weight (Mw, kDa) and isoelectric point (pI) of all putative proteins. Prediction of the transmembrane domains in all AMT proteins was finished with TMHMM Server version 2.0 (http://www.cbs.dtu.dk/services/TMHMM/, accessed on 24 June 2021).

2.2. Phylogenetic Analysis, Gene Structures and Genomic Locations

After being downloaded from the NCBI protein database, the protein sequences in full length for *A. thaliana*, *Oryza sativa*, *P. trichocarpa*, *Sorghum bicolor*, *Lycopersicon esculentum*, *Glycine max* and *Lotus japonicas* were researched for their evolutionary relationships. Multiple alignments were executed based on default parameters in the DNAMAN program (Lynnon Biosoft, San Ramon, CA, USA). The MEGA6 program was employed for plotting phylogenetic trees by virtue of the Neighbor-Joining (NJ) method with Poisson corrections and 1000 replicates for the bootstrap analysis. Through the method for coding sequences and genomic sequences, a scattergram of exon/intron arrangement was acquired from the online Gene Structure Display Server (http://gsds.cbi.pku. edu.cn/, accessed on 24 June 2021). Moreover, the sequence logos of AMT subfamilies were generated using WEBLOGO (http://weblogo.berkeley.edu/logo.cgi, accessed on 24 June 2021). Chromosomal locations were retrieved from the Genome Database for Rosaceae (GDR;

http://www.rosaceae.org/, accessed on 24 June 2021). Additionally, mapping of genes to the chromosomes was completed via MapDraw [23].

2.3. Analysis on Phosphorylation of Residues within the C-Terminal Cytoplasmic Tail

Possible phosphorylation sites were recognized by scanning the sequences of the MdAMT proteins with the NetPhos program (http://www.cbs.dtu.dk/services/NetPhos/, accessed on 24 June 2021), and homologies of the known phosphorylation sites were then discovered by integration with the aligning of the AtAMT1;1 sequence.

2.4. Analysis on Putative Cis-Elements of AMT Genes in Apple

To probe into cis-elements in the promoter region of *MdAMT* genes, the PLACE online server (http://www.dna.affrc.go.jp/PLACE/, accessed on 24 June 2021) was employed for prediction of putative cis-elements of *MdAMT* genes after downloading single genomic DNA sequences (2 kb) upstream of the initiation codon (ATG) from the apple genome database.

2.5. Transcription Modes of AMT Genes in Multifarious Tissues and Diurnal Rhythms

To analyze the tissue-specific expression of apple AMTs, we used *M. domestica* 'Golden delicious' 6-year-old trees growing at the Horticultural Experimental Station of Northwest A&F University (Yangling, Shaanxi, China). New roots, young stems, shoot tips, mature leaves and young fruits were sampled at 16 days after blooming (DAB), while flowers and mature fruits were sampled at 5 DBA and 122 DAB, respectively. All samples were harvested from the south side of the tree canopy at 10:00–11:00 a.m., under full sun light exposure. Moreover, with respect to experiments of light regime, samples of mature foliage and new roots were taken at 6:00, 10:00, 14:00, 18:00 and 22:00 during the same day.

2.6. Plant Growth and Treatments

Seedlings of *Malus hupehensis* growing at the Horticulture Experimental Station were used for the N-dependent and osmotic treatments. Briefly, similarly sized seedlings (8–10 foliage, roughly 15 cm tall) were moved to plastic vats containing 14 L of modified Hoagland's nutrient solution (1 mM NO_3NH_4 as N source) of half strength, and put in a growth cabinet (23–25 °C/15–18 °C day/night), with light from sodium lamps during the 14 h daylight. The nutrient solution was aerated each hour with an air pump. Moreover, the adjustment of pH to 5.8–6.0 was accomplished with H_2SO_4, and refreshment of each solution was completed every four days. The seedlings were ready for treatment after 10 days of such pre-cultivation.

For the N-dependent experiment, the seedlings were cultured under N-free conditions for 2 days, followed by 2 days of cultivation in nutrient solution with ammonium as the unique N source. Roots and leaves were sampled at 0 h, 6 h and 48 h, respectively. The osmotic stress was induced by supplying 5% PEG6000 to the nutrient solution. The seedlings were treated with PEG for 24 h, then transferred to a PEG-free nutrient solution. Samplings of roots were collected at 0 h, 1 h, 6 h and 24 h during PEG treatment, and 1 h, 24 h after transferred to PEG-free nutrient solution, respectively.

2.7. RNA Segregation and Quantitative RT–PCR Analysis

Following extraction of total RNA as per the CTAB method [24], the quantity and quality of RNA were checked using a NanoDrop 2000c spectrophotometer (Thermo Scientific, Waltham, MA, USA) and agarose gel electrophoresis. Removal of surplus DNA was conducted by means of processing with RNase-free DNase I (Invitrogen, Carlsbad, CA, USA). Thereafter, first-strand cDNA was synthesized from 1 μg total RNA using a SYBR® PrimeScript™ RT-PCR Kit II (TaKaRa, Dalian, China), followed by quantitative reverse transcription PCR (qRT-PCR) on an iQ5.0 instrument (Bio-Rad, Hercules, CA, USA) for measurement of the expression features of *MdAMTs*. With gene-specific primers designed using the Primer Premier 5.0 software, the primer sequences are stated in Table S1. The

real-time PCR was carried out under the reaction program as previously described [25]. Each PCR was conducted in a 20 µL reaction volume, which contained 10.0 µL of SYBR® Premix Ex Taq™ (TaKaRa, Japan), 1.0 µL of cDNA template, 0.4 µL of each specific primer and 8.2 µL of ddH_2O. The PCR conditions involved an initial 95 °C for 5 min; then 40 cycles of 95 °C for 10 s, 60 °C for 30 s and 72 °C for 30 s. The *EF-1α* gene (DQ341381) was selected as a reference gene. To minimize inherent errors, each qRT-PCR was accomplished 3 times on 3 separate RNA extracts from 3 biological replicates. The relative content of *MdAMT* genes was found using the $2^{-\triangle\triangle CT}$ method [26].

2.8. Functional Analysis in Yeast

The recombinant plasmid pYES2-*AMT1;2* was built by cloning the CDS region of the *AMT1;2* gene into the pYES2 vector, with the KpnI and XbaI sites incorporated into the primers. Specific primers for gene cloning are listed in Table S1. Yeast strain 31019b was unable to germinate on the medium containing less than 5 mM NH_4^+, as the unique N source was transformed with pYES2 or pYES2-*AMT1;2* [27]. Yeast complementation assays were carried out as described antecedently [28]. Single colonies were precultured in a liquid YNB medium in an agitation incubator at 30 °C until the OD600 reached 0.5–0.6. Cells were collected and resuspended in sterile water to a final OD600 of 1.0 before being diluted serially by a factor of 10. For complementation tests, 5 µL aliquots of yeast cell suspensions from each dilute were spotted on YNB plates supplemented with 0.02, 0.2 or 2 mM NH_4Cl, respectively, as the sole N source at pH 5.8. Image taking was completed 3 days after incubation at 30 °C.

3. Results

3.1. Identification and Chromosomal Location of AMT Genes in Apple

In total, 15 putative AMT proteins and the related encoding genes were ultimately recognized from the apple genome (Table 1), with a length of 431–534 amino acids (a.a.) for encoded proteins. According to prediction, these AMTs had isoelectric points (pI) of 5.10–8.77, with 6.91 on average, and molecular weights of 47.7–57.15 kDa, with a mean of 52.45 kDa. In addition, transmembrane domains in AMT proteins were predicted, and it was uncovered that each domain incorporated 9–11 transmembrane helices (TMHs), which was consistent with the discoveries in other plant species.

Table 1. Features of AMT family members in apple.

Gene	Locus	Genomic Position	CDS Length	Protein Size	pI	MW (kDa)	TMHs
MdAMT1.1	MDP0000427102	chr17:14131094-14132698	1605	534	6.34	57.15	11
MdAMT1.2	MDP0000572721	chr13:7142043-7143557	1515	504	6.55	54.12	11
MdAMT1.3	MDP0000266406	chr13:27756622-27758139	1518	505	7.62	53.74	11
MdAMT1.4	MDP0000909614	chr5:15840835-15842328	1494	497	6.82	52.88	9
MdAMT1.5	MDP0000182546	chr13:27756243-27757760	1518	505	7.19	53.72	11
MdAMT1.6	MDP0000518257	chr3:6372147-6373547	1401	466	5.10	50.13	10
MdAMT1.7	MDP0000240418	chr3:6371890-6373290	1401	466	5.10	50.13	10
MdAMT1.8	MDP0000289954	chr11:6610329-6611729	1401	466	5.18	50.06	9
MdAMT2.1	MDP0000650358	chr4:16260628-16264571	1473	490	8.46	52.82	11
MdAMT2.2	MDP0000137929	chr12:24732899-24735197	1473	490	8.66	52.69	11
MdAMT3.1	MDP0000245173	chr15:7176000-7180690	1467	488	6.78	52.68	11
MdAMT4.1	MDP0000268493	chr8:17433482-17435888	1503	500	8.77	54.52	9
MdAMT4.2	MDP0000177077	chr15:5549862-5551942	1455	484	8.17	52.72	11
MdAMT4.3	MDP0000186795	chr11:31604485-31607250	1416	471	6.24	51.58	10
MdAMT4.4	MDP0000211452	chr2:10641333-10643931	1296	431	6.70	47.77	9

The genomic distribution of *AMTs* was ascertained by retrieving chromosomal locations of each recognized sequence from the apple genome database. It was discovered that the 15 *AMTs* were distributed on 10 of the 17 chromosomes in apple, with three on Chr 13; two each on Chr 3, 11 and 15; and one each on Chr 2, 4, 5, 8, 12 and 17 (Figure 1).

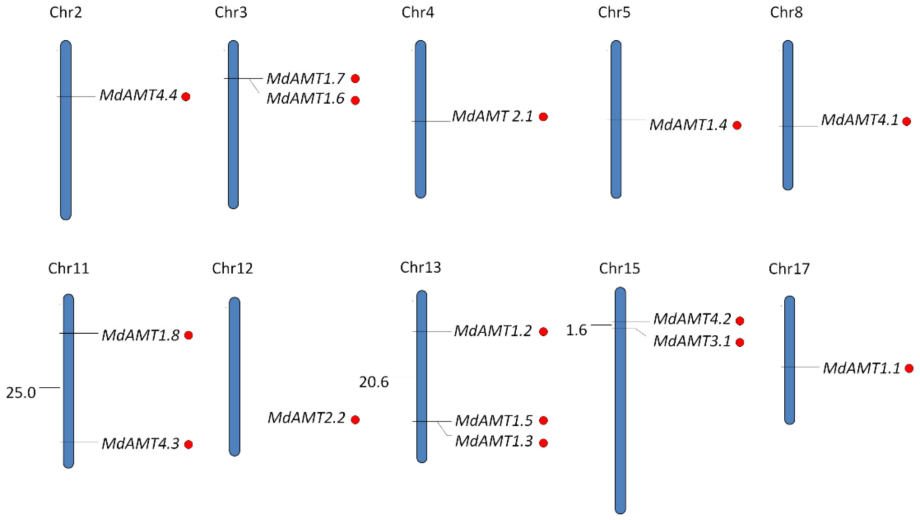

Figure 1. Locations of *AMT* gene family members on chromosomes in apple.

3.2. Phylogenetic Analysis and Gene Structure of AMT Genes

Following alignment of the protein sequences in full length from eight different plant species (Figure 2), a phylogenetic tree was built through the Neighbor-Joining method using MEGA6 software to appraise the evolutionary connections among *AMT* family members. Two major clades and four clusters were uncovered. Among 15 *AMT* genes in apple, 8, 2 and 1 were separately in the *AMT1, AMT2* and *AMT3* clusters, and the remaining *AMTs* were in *AMT4* cluster.

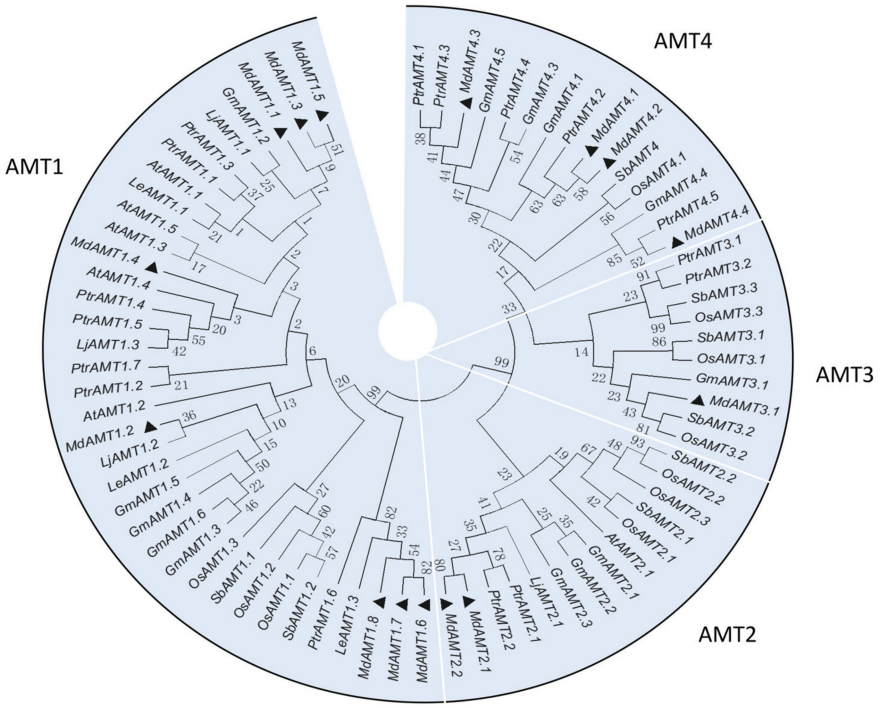

Figure 2. Phylogenetic tree of AMT gene-encoded proteins from Arabidopsis thaliana, Oryza sativa, Populus trichocarpa, Sorghum bicolor, Lycopersicon esculentum, Glycine max, Lotus japonicas and Malus domestica. The phylogenetic tree was plotted with MEGA6 using the N-J method, with 1000 bootstrap replicates.

Based on a multiple protein sequence alignment of 15 AMTs, the building of an unrooted phylogenetic tree was finished (Figure 3A). The exon/intron structure revealed

that the *AMT* genes in the same cluster displayed alike exon/intron structure and number (Figure 3B). For *AMT1* subfamily members, none of the sequences contained introns, but *AMT2* subfamily members comprised 2–4 introns with different intron phases and distinctly varied lengths. Amino acid sequence alignment of AMTs revealed that all of them contained the highly conserved AMT-specific domain (Figure S1). The sequence logos of the AMT1 and AMT2 subfamilies were presented in Figure 3C.

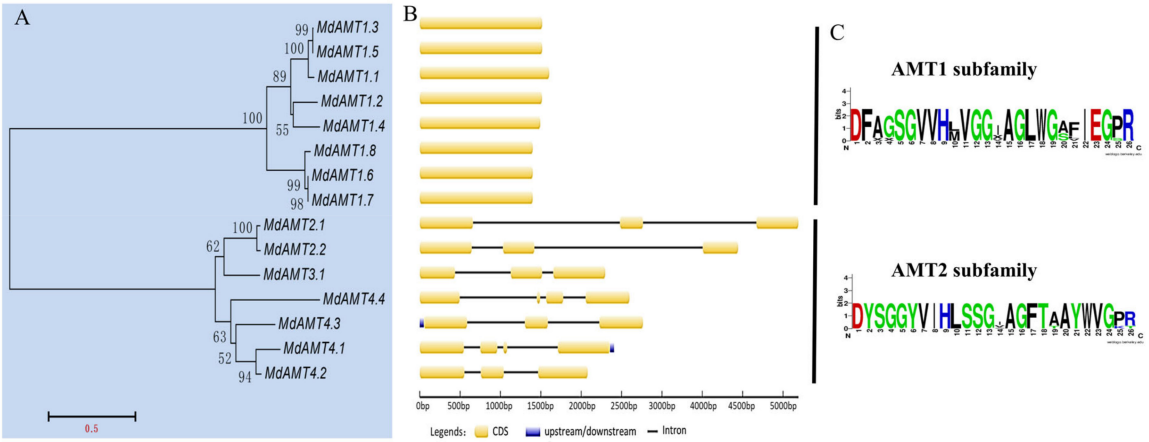

Figure 3. Paralog phylogenetic tree, gene structure and conserved domains of the AMT gene family in apple. (**A**) Phylogenetic tree built using MEGA6 by means of the N-J method, with 1000 bootstrap replicates. (**B**) Gene structure of MdAMT genes, where yellow boxes and gray lines separately stand for exons and introns. (**C**) Conserved domains delimiting the AMT subfamilies generated using WEBLOGO (http://weblogo.berkeley.edu/logo.cgi, accessed on 24 June 2021).

3.3. Analysis on Phosphorylation of Residues within the C-Terminal Cytoplasmic Tail

Previous studies have reported seven phosphorylation sites (T460, S475, S488, S490, S492, T496 and T497) within the C-terminal tail of AtAMT1.1 in *Arabidopsis* [29,30]. According to the prediction of possible phosphorylation residues within the C-terminal cytoplasmic tail of AMT proteins with the NetPhos program, a homologue of AtAMT1.1 T460 was discovered in five MdAMT1 proteins (Figure 4), signifying that apple may experience a like regulation by phosphorylation in *Arabidopsis*. Furthermore, another two potential phosphorylation sites more highly conserved within the C-terminal region were also recognized, which were homologous to AtAMT1.1 S449 in OsAMT1 and AtAMT1.1 T477 in OsAMT2, respectively, indicated by boxes (Figure 4). Nevertheless, the potential phosphorylation sites mentioned above are deserving of investigation in apple.

3.4. Expression Profiles for AMT Genes in Different Tissues

To investigate the transcription patterns of apple *AMT* genes, their expression in mature leaves, stems, shoot tips, roots, flowers and young fruits was examined (Figure 5). In fact, transcripts of 10 *AMT* genes: *AMT1;1/1;2/1;5/1;6/1;8/2;1/2;2/3;1/4;2/4;3* were detected; for the rest, *AMT*s showed relatively low transcript levels in the tested tissues. The expression levels of *AMT3;1* were detected mostly in roots and leaves (Figure 5A). Among the *AMT* family members, *AMT1;2* showed relatively high transcript levels in roots. *AMT2;1* and *AMT2;2* exhibited the strongest expression levels in roots, and *AMT2;1* also showed high expression levels in stems. In addition, *AMT4;2/4;3* were root-specific transcribed (Figure 5B). *AMT1;1/1;5/1;6/1;8* were expressed in all tested tissues, and *AMT1;5/1;6* manifested high transcript levels in mature leaves and young fruits. In fruits, transcript abundance of *AMT1;1/1;6/1;8* decreased during fruit ripening, except for *AMT1;5*, which was up-regulated at an early stage during fruit development, and then down-regulated until fruits were fully matured at 128 DBA (Figure 5C).

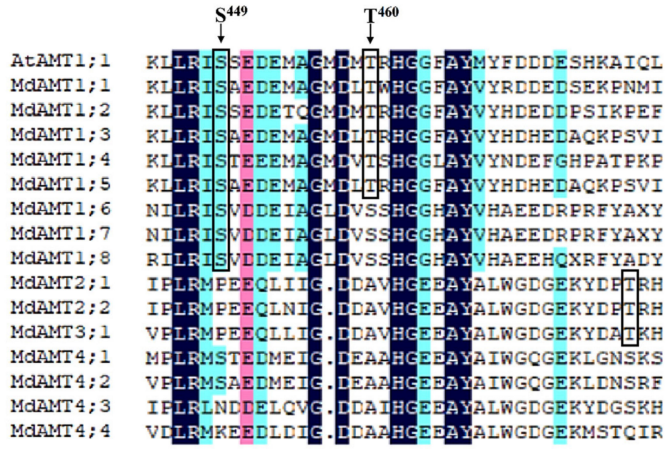

Figure 4. Phosphorylation sites conserved within the C-terminal region of MdAMT proteins. For the recognition of possible phosphorylation sites, the NetPhos program was adopted, with sites conserved within phylogenetic groups indicated by boxes.

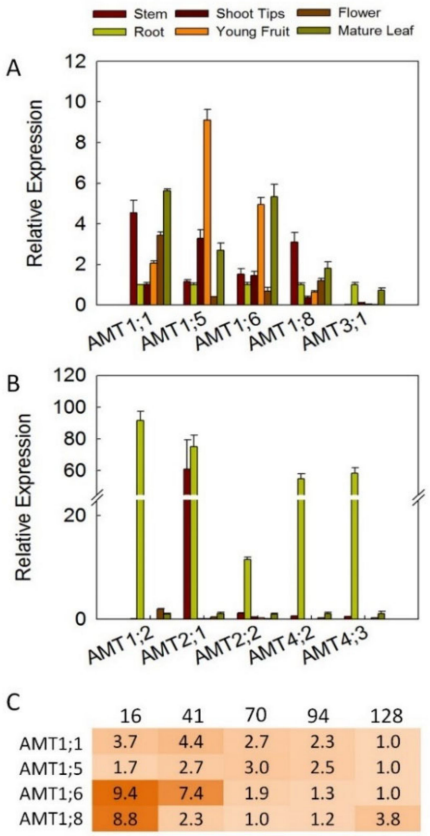

Figure 5. Relative transcript levels of *AMT* genes in diverse tissues of apple. *AMT1;1/1;5/1;6/1;8/3;1* (**A**) and *AMT1;2/2;1/2;2/4;2/4;3* (**B**) distributed in roots, stems, shoot tips, young fruits, flowers and mature leaves. (**C**) Transcript levels of *AMT1;1/1;5/1;6/1;8* in fruits at 16, 41, 70, 94, 128 DBA. Normalization of data to expression level of EF-1α was conducted. With regard to each sample, mean value of three replicates is taken. Vertical bars indicate standard deviation. DBA, day after bloom.

3.5. Transcription Modes of AMT Genes during Diurnal Rhythms

To find out the expression modes of *AMTs* during diurnal cycles, the expression levels of *AMTs* in roots and foliage sampled at 4 h intervals were measured (Figure 6). Our data indicated that transcript levels of *AMT1;1/1;2/1;6* exhibited diurnal rhythms in roots (Figure 6A). The expression levels of *AMT1;1/1;6* were strongest at 18:00 in roots, while the

highest transcript abundance of *AMT1;2* was found at 10:00. In leaves, it was discovered that *AMT1;2/2;1/2;2* experiences the largest diurnal changes in transcript levels (Figure 6B). Interestingly, similar trends was found between *AMT2;1* and *AMT2;2*, with the Pearson correlation coefficient value of 0.982 (p = 0.003), showing a significant positive correlation between expression levels of *AMT2;1* and *AMT2;2* during diurnal cycles (Table S2). The transcript levels of *AMT2;1* and *AMT2;2* showed an increase trend with the highest expression levels being found at 22:00. In addition, the expression levels of the remaining *AMT*s did not show obvious diurnal changes.

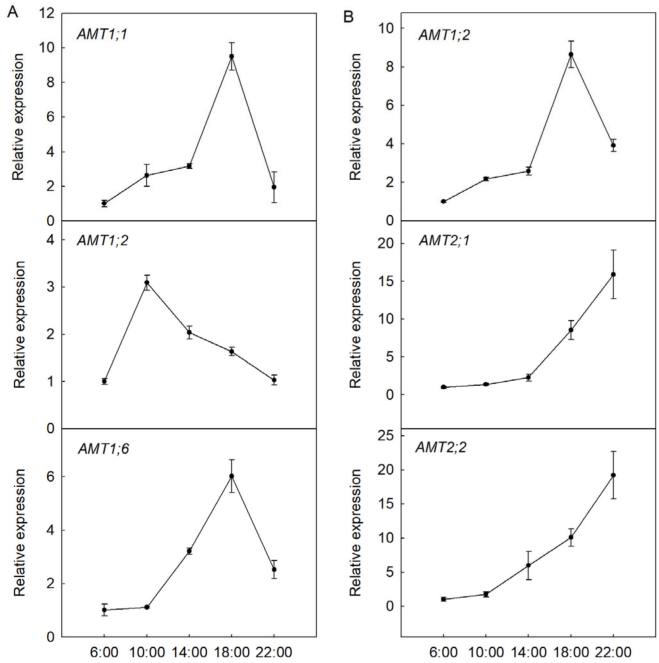

Figure 6. Effect of diurnal rhythms on *AMT* expression in roots (**A**) and leaves (**B**) of apple.

3.6. Impact of N-Starvation and Ammonium Resupply on Expression Profiles of AMT Genes

The transcription patterns of apple *AMT*s under N-dependent treatment were also examined (Figure 7). In roots of seedlings under N-starvation conditions, *AMT1;2/1;5* were on the rise at 6 and 48 h, while the transcript abundance of *AMT1;1* changed little. *AMT1;6/1;8/2;1/2;2/4;3* were down-regulated at 6 h, and then were on the rise at 48 h. The expression levels of *AMT3;1* were unaltered at 6 h, then increased at 48 h. *AMT4;2* was on the decline at 6 h and remained unchanged until 48 h (Figure 7A). In leaves of N-starved seedlings, *AMT2;2* was greatly up-regulated, while *AMT2;1* was on the decline at 6 and 48 h. Additionally, *AMT1;1/1;6* manifested slightly increased transcript levels at 6 and 48 h, while *AMT1;2* changed little in response to N starvation. The transcript levels of *AMT1;5/3;1* decreased at 6 h, then increased at 48 h (Figure 7B).

In roots of seedlings under NH_4^+-resupply conditions, *AMT1;2* was up-regulated slightly at 6 h and 48 h. *AMT1;5/1;6/1;8/2;2/3;1/4;2* were on the decline at 6 and 48 h, while *AMT2;1/4;3* were on the decline at 6 h and remained unchanged at 48 h. *AMT1;1* experienced unchanged transcript abundance at 6 h and then dropped transcript abundance at 48 h (Figure 7A). In the foliage of seedlings receiving NH_4^+ resupply, *AMT1;1/1;2* were on the decline at 6 and 48 h, and *AMT1;5/3;1* also decreased at 6 h, but remained unchanged at 48 h. The transcript levels of *AMT2;1* remained unchanged at 6 h and decreased at 48 h. *AMT2;2* was on the decline at 6 h, then up-regulated at 48 h. In addition, the transcript abundance of *AMT1;6* was not altered by NH_4^+ resupply (Figure 7B).

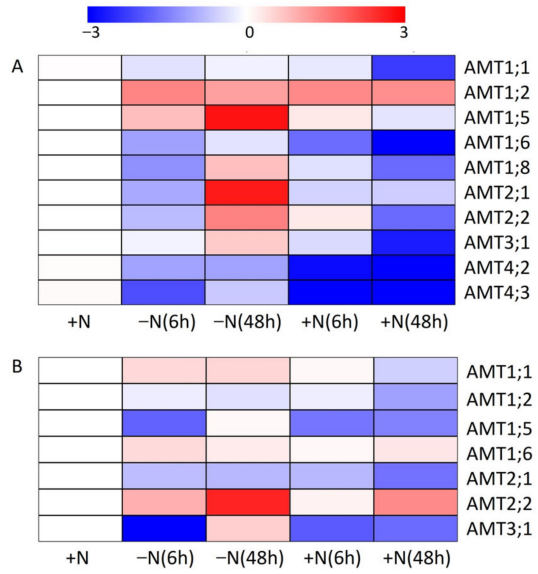

Figure 7. Expression profiles of apple *AMT* genes in roots (**A**) and leaves (**B**) under N-starvation and ammonium resupply conditions. The seedlings of *M. hupehensis* were cultured under N-free conditions for 2 days, followed by 2 days of cultivation in nutrient solution with ammonium as the only N source. Sampling of roots and leaves was accomplished at 0 h, 6 h and 48 h, respectively.

3.7. Effects of Osmotic Stress on Expression Patterns of AMT Genes

We also investigated the transcription patterns of *AMTs* in the reaction to osmotic stress (Figure 8). In the roots of stressed seedlings, most investigated *AMT*s were up-regulated at 1 h, except for *AMT1;2/3;1*, which were down-regulated at 1 h, 6 h and 24 h. The transcript abundance of *AMT1;1/1;5* continued to increase, while expression levels of *AMT2;1/4;3* decreased notably at 6 h and 24 h. For *AMT1;6*, the expression levels increased at 6 h and then decreased at 24 h. In addition, the transcript levels of *AMT1;8/2;2* changed little at 6 h and 24 h. When the stressed seedlings transferred to normal conditions, *AMT1;1/1;5/1;6* were then on the decline at 1 h and 24 h. For the remaining *AMT*s, enhanced transcript levels were found at 1 h after short-term osmotic stress. Almost all the investigated *AMT*s were down-regulated at 24 h, except for *AMT1;2*, the expression levels of which remained unchanged.

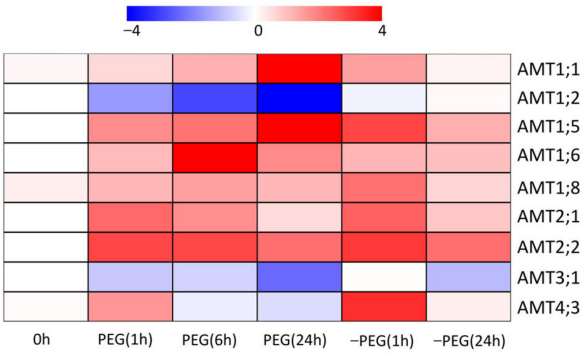

Figure 8. Impacts of osmotic stress on expression patterns of apple *AMT* genes. The osmotic stress was generated by supplying 5% PEG6000 to the nutrient solution. Root samples were collected at 0 h, 1 h, 6 h and 24 h during PEG treatment, and 1 h and 24 h after being transferred to PEG-free nutrient solution. TBtools was used to generate the heat map. Scale bars represent the log2 normalized expression. Red indicates higher expression, while blue indicates lower expression.

3.8. Functional Analysis of AMT1;2 in an Ammonium Uptake-Deficient Yeast Mutant

Among the apple *AMT* genes, *AMT1;2* showed high expression levels in roots and was quite sensitive to plant N status and osmotic stress. To elucidate the underlying role of apple *AMTs*, functional complementation of *AMT1;2* was further carried out with yeast mutant strain 31019b defective in ammonium uptake. After transforming cells of the yeast strain 31019b with *AMT1;2* or empty vector pYES2, growth complementation on YNB plates with 0.02, 0.2 or 2.0 mM NH_4Cl added as the sole N source was examined. There was growth under submillimolar ammonium as the sole N source by expression of *AMT1;2* in 31019b cells (Figure 9). Additionally, cells transformed with empty pYES2 vector, acting as a negative control, showed no growth. These results showed that the defective yeast strain 31019b could be functionally complemented by *AMT1;2*, indicating that *AMT1;2* functions in NH_4^+ transport.

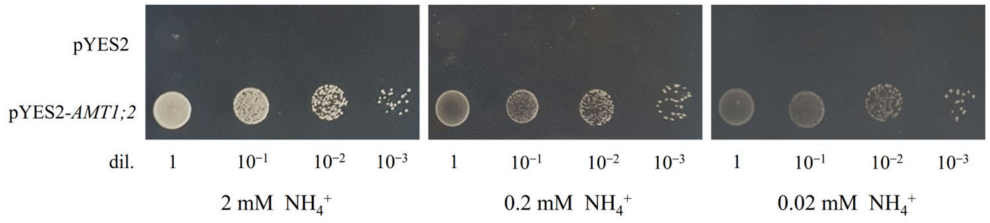

Figure 9. Functional analysis of *AMT1;2* in yeast. Yeast strains 31019b transformed with pYES2 or pYES2-*AMT1;2* developed on YNB medium, with 0.02, 0.2 or 2.0 mM NH_4Cl added as the sole N source at pH 5.8, with dilution factors of spotted cells displayed at the bottom. Photographs were taken after 3 days growing at 30 °C.

4. Discussion

The AMTs, major high-affinity NH_4^+ transporters in plants, mediate the transmembrane uptake of ammonium [7]. After the first plant *AMT* gene was recognized from *Arabidopsis* by means of functional complementation of a yeast mutant with deficient uptake of ammonium [31], several *AMTs* were discovered and characterized in various plant species [6,10,22,32]. In this work, 15 *AMTs* were retrieved from the apple genome and assigned to the following two subfamilies—*AMT1* and *AMT2*—with the latter further divided into three subclades (Figure 2), which was consistent with previous studies in rice, poplar and peach [6,8,32]. Moreover, *AMT* genes in the same cluster manifested alike exon/intron structures, with no intron in *AMT1* subfamily members and 2–4 introns in *AMT2* subfamily members (Figure 3). Consistent discoveries have also been reported in other plant species [6–8]. Similar to poplar, apple possessed many more *AMT2* genes than *Arabidopsis* and more *AMT1* genes than rice (Figure 2), signifying function redundancy of apple *AMTs* or execution of a special function leaning on varying tissue expression. Multiple forms of ammonium transporters in woody plants allow a greater regulatory flexibility and enable cells to take up ammonium over a wide range of concentrations.

Expression features of apple *AMTs* demonstrated intricate tissue specificities, indicating that they may play distinct physiological functions in ammonium uptake and utilization. We detected high transcript levels of *AMT1;2/2;1/2;2/4;2/4;3* in roots (Figure 5), and suspected that they may play roles in ammonium uptake from the soil under various environmental conditions. In *Arabidopsis*, *AtAMT1;1/1;2/1;3* were mainly expressed in roots and contributed to 30%, 18–26%, and 30–35% of the high-affinity ammonium uptake ability in roots, respectively [7,10]. *AtAMT2* manifested transcript abundances preferentially centered on the pericycle and was responsible for ammonium loading in xylem [33]. In this study, *AMT1;1/1;8/2;1* showed relatively high expression levels in stems and possibly functioned in the ammonium transport from roots to new branches (Figure 5). In addition, *AMT1;1/1;5/1;6* displayed relatively high transcript levels in foliage, suggesting that they may be active in the retrieval from the apoplast of foliage [34] or retrieval from senescent foliage to young foliage [6]. Moreover, there is a significant influence of N

transport to reproductive organs on flower set, fruit development and seed production [35]. In *Arabidopsis*, *AtAMT1;4* had a specific expression in pollen and mediated ammonium transport into the pollen [36]. Previous studies have also detected the transcript levels of *LjAMT1;1-1;3* in flowers [37] and *ZmAMT1.1a* in seeds [22]. In this work, we observed that *AMT1;1/1;5/1;6/1;8* were expressed in flowers and fruits (Figure 5). It is worth noting that *AMT1;5* had the highest transcript levels in young fruits and was up-regulated at an early stage, suggesting that it may play roles in providing ammonium nutrition during fruit development. Farther functional analysis is called for to find out the precise function of *AMT*s and their connections with reproductive organ development in plants.

Additionally, the transcript abundance of *AMT1;1/1;2/1;6/2;1/2;2* in roots or leaves of apple trees exhibited diurnal rhythms (Figure 6). For instance, the transcript levels of *AMT2;1/2;2* increased during a diurnal cycle with the highest expressions levels being found at 22:00, which was similar to *PtrAMT1;6* in poplar [6]. Under a day/night cycle, *LeAMT1;2* showed the highest transcript level in the night cycle, but *LeAMT1;3* reached uppermost transcript abundance at the outset of light [34]. Moreover, diurnal rhythms of *AMTs* were also found in rice [38] and cabbage [39]. Consistently, cis-acting element analysis in this work demonstrated that the circadian elements involved in circadian control were noticed in the promoter regions of most investigated *MdAMT* genes (Table S1).

The regulatory characteristics of *AMT*s may vary depending on plant species when subjected to different N regimes. It has been shown in research on *Arabidopsis* that there was enhancement in high-affinity ammonium uptake capacity in roots in the case of N limitation [7,29], and increment in *AtAMT1;1* was not contingent on a local ammonium signal but rather on local or systemic N inadequacy [40]. Similar to *AtAMT1;1*, *AMT1;2/1;5* were significantly induced by N deprivation in roots (Figure 7). *AMT1;8/2;1/2;2* also manifested high transcripts after N starvation for 48 h, suggesting that the apple *AMTs* mentioned above may be controlled by systematic N signal and regulated by the whole-plant N status. In contrast, decreased transcript abundance of plant *AMTs* during N starvation periods have also been reported, including *OsAMT1;2*, *ZmAMT1;1a* and *ZmAMT1;3* [22,32]. Furthermore, *ZmAMT1;1a* and *ZmAMT1;3* displayed rapidly increased transcript abundance after ammonium resupply to N-deprived maize seedlings, and proved to be controlled specifically by a local ammonium signal [22]. However, most investigated *AMTs* were down-regulated under ammonium resupply condition, except for *AMT1;2* in roots (Figure 7). *PbAMT1;5* displayed repressed transcription after 2.5 mM NH_4Cl was resupplied following N deprivation [41]. Taken together, plant *AMT* genes showed multiple transcript patterns to N regimes, so as to optimize ammonium acquisition from a wide range of external N concentrations.

Previous studies have shown that ammonium nutrition seems to be positively active in the plant tolerance to osmotic stress [14,15,19]. Therefore, we analyzed the transcription patterns of apple *AMTs* and found that most investigated *AMTs* were up-regulated when subjected to short-term osmotic stress, except for *AMT1;2/3;1* (Figure 8), indicating that these *AMTs* were quite responsive to osmotic stress. Similarly, *M. hupehensis* seedlings presented comparatively enhanced ammonium uptake, with notably increased expression levels of *AMT4;2* and *AMT4;3* in acclimating to PEG-induced osmotic stress [18]. Consistent discoveries have also been noticed in *P. simonii* and *Malus prunifolia* [19,42]. Furthermore, ammonium is also efficient in assuaging the adverse effect of salinity [16,17,43]. It is worth noting that a series of cis-elements responsive to abiotic stress were distributed in the promoter region of *MdAMTs*, including heat stress responsiveness, low-temperature responsiveness, dehydration responsiveness, anaerobic induction and wound responsiveness (Table S2), further suggesting that transcriptional regulation of *AMTs* may be active in plant tolerance to various abiotic stresses. Therefore, further research is requisite to figure out the functional characteristics and regulation mechanisms of *AMT*s in response to various abiotic stresses.

In addition to transcriptional regulation, plant AMTs also go through posttranslational regulation in reaction to altering ammonium concentrations. When external ammonium

supplies are elevated, symptoms of toxicity are noticed in most higher plants [44]. To prevent cellular ammonium toxicity, ammonium transport is controlled by ammonium-triggered feedback suppression. In *Arabidopsis*, phosphorylation sites have been recognized in some AMT proteins, including AtAMT1.1 [12,13,45]. The T460 phosphorylation-induced rapid shut off of AtAMT1;1, in particular, is regarded as vital for preventing ammonium toxicity [29]. It has been confirmed that the phosphorylation state of T460 placed in the C-terminus conserved domain is requisite for the functional shift of AtAMT1;1 and may be of universal significance in AMT proteins [30]. When compared with AtAMT1;1, the conserved T460 phosphorylation site was found in most apple AMT1 subfamily members (Figure 4), indicating that phosphorylation at a specific site of apple AMT1 is possibly of equivalent significance for preventing ammonium toxicity and regulating ammonium uptake under various environment conditions. Given that the T460 site was non-conservative in AMT2 subfamily members, there may be dissimilar modulation mechanisms between members of AMT1 and AMT2 subfamilies. Nonetheless, several phosphorylation residues were noticed in this work, and further surveys on phosphorylation of apple AMTs are worthy of our attention.

In general, functional study of plant *AMT* genes is mainly conducted by means of yeast functional complementation, oocyte two-electrode voltage clamp electrophysiology and plant-level genetic manipulation [30]. Previous yeast heterologous expression studies have indicated that plant AMT1 genes encode high affinity transporters [7,28]. In our study, analysis of *AMT1;2* activity was completed by means of complementation of the yeast strain 31019b with insufficient ammonium uptake. Normal growth of yeasts of this strain expressing recombinant pYES2-*AMT1;2* was discovered on a solid medium with 2 mM NH_4^+ added as the unique N source (Figure 9), implying that *AMT1;2* is active in NH_4^+ transport. Additionally, *AMT1;2* mainly existed in roots and could be induced by N deficiency; it might take part in high affinity NH_4^+ uptake from soil in apple. Further research concerning functional characteristics and the molecular mechanism of apple *AMTs* is still required.

5. Conclusions

In this work, we identified and characterized in silico 15 *AMTs* from the apple genome, which could be divided into AMT1 and AMT2 subfamilies, with highly similar conserved domain and exon–intron structure within the same subfamilies. Expression features demonstrated that some *AMT* genes were preferentially expressed in specific tissues and may participate in ammonium transport into specific tissues and organs. We speculated that *AMT1;5* may play roles in providing ammonium nutrition during fruit development. In addition, apple *AMTs* showed multiple transcript patterns of N-starvation and ammonium resupply, which may allow plants to respond differentially to varying nutritional conditions in the environment. Furthermore, up-regulation of most investigated *AMTs* was found in response to PEG-induced osmotic stress, suggesting that transcriptional regulation of apple *AMTs* may be involved in plant tolerance to various abiotic stress. Therefore, more research is necessary to figure out the biological functions and regulatory mechanisms of *AMTs* when plants are exposed to various environmental conditions.

Supplementary Materials: The following supporting information can be downloaded at: https://www.mdpi.com/article/10.3390/horticulturae8050457/s1, Figure S1: Multiple sequence alignment of MdAMTs; Table S1: Primer sequences used in this work; Table S2. Correlation analysis of *AMT2;1* and *AMT2;2* expression levels during diurnal cycles. Table S3: Analysis of cis-acting elements that existed in the promoters of *MdAMT* genes.

Author Contributions: Conceptualization, L.H. and F.M.; data curation, L.H. and J.L.; formal analysis, L.H., J.L. and B.Z.; writing—original draft preparation, L.H.; writing—review and editing, Y.H. and F.M. All authors have read and agreed to the published version of the manuscript.

Funding: This work was supported by the Scientific and Technological Innovation Programs of Higher Education Institutions in Shanxi (No. 2019L0358); the PhD Start-up Fund of Shanxi Province (No. SXYBKY2018014); the Technology Innovation Fund of Shanxi Agricultural University (No. 2018YJ03, 2016ZZ01) and the Open Project of State Key Laboratory of Crop Stress Biology for Arid Areas (No. CSBAA2019013).

Institutional Review Board Statement: Not applicable.

Informed Consent Statement: Not applicable.

Acknowledgments: We thank Yuan Lixing (College of Resources and Environmental Sciences, China Agricultural University) for kindly providing the ammonium uptake-deficient yeast strain 31019b.

Conflicts of Interest: The authors declare no conflict of interest.

References

1. Khasawneh, A.; Alsmairat, N.; Othman, Y.A.; Ayad, J.Y.; Al-Qudah, T.; Leskovar, D.I. Influence of nitrogen source on physiology, yield and fruit quality of young apricot trees. *J. Plant Nutr.* **2021**, *44*, 2597–2608. [CrossRef]
2. Nava, G.; Dechen, A.R.; Nachtigall, R.G. Nitrogen and potassium fertilization affect apple fruit quality in Southern Brazil. *Commun. Soil Sci. Plant Anal.* **2007**, *39*, 96–107. [CrossRef]
3. Yamasaki, A.; Yano, T. Effect of supplemental application of fertilizers on flower bud initiation and development of strawberry-possible role of nitrogen. *Acta Hortic.* **2009**, *842*, 765–768. [CrossRef]
4. Bloom, A.J.; Sukrapanna, S.S.; Warner, R.L. Root respiration associated with ammonium and nitrate absorption and assimilation in barley. *Plant Physiol.* **1992**, *99*, 1294–1301. [CrossRef]
5. Britto, D.T.; Kronzucker, H.J. NH_4^+ toxicity in higher plants: A critical review. *J. Plant Physiol.* **2002**, *159*, 567–584. [CrossRef]
6. Couturier, J.; Montanini, B.; Martin, F.; Brun, A.; Blaudez, D.; Chalot, M. The expanded family of ammonium transporters in the perennial poplar plant. *New Phytolo.* **2007**, *174*, 137–150. [CrossRef]
7. Yuan, L.X.; Loqué, D.; Kojima, S.; Rauch, S.; Ishiyama, K.; Takahashi, H.; Von Wirén, N. The organization of high-affinity ammonium uptake in *Arabidopsis* roots depends on the spatial arrangement and biochemical properties of AMT1-type transporters. *Plant Cell* **2007**, *19*, 2636–2652. [CrossRef]
8. Tang, M.; Li, Y.; Chen, Y.; Han, L.; Zhang, H.; Song, Z. Characterization and Expression of Ammonium Transporter in Peach (*Prunus persica*) and Regulation Analysis in Response to External Ammonium Supply. *Phyton* **2020**, *89*, 4. [CrossRef]
9. Ludewig, U.; Wilken, S.; Wu, B.; Jost, W.H.; Obrdlik, P.; Bakkoury, M.E.; Marini, A.; André, B.; Hamacher, T.; Boles, E.; et al. Homo- and hetero-oligomerization of ammonium transporter-1 NH_4^+ uniporters. *J. Biol. Chem.* **2003**, *278*, 45603–45610. [CrossRef]
10. Loqué, D.; Yuan, L.; Kojima, S.; Gojon, A.; Wirth, J.; Gazzarrini, S.; Ishiyama, K.; Takahashi, H.; Von Wirén, N. Additive contribution of AMT1;1 and AMT1;3 to high-affinity ammonium uptake across the plasma membrane of nitrogen-deficient *Arabidopsis* roots. *Plant J.* **2006**, *48*, 522–534. [CrossRef]
11. Konishi, N.; Ma, J. Three polarly localized ammonium transporter 1 members are cooperatively responsible for ammonium uptake in rice under low ammonium condition. *New Phytolo.* **2021**, *232*, 1778–1792. [CrossRef]
12. Loqué, D.; Lalonde, S.; Looger, L.L.; Von Wirén, N.; Frommer, W.B. A cytosolic trans-activation domain essential for ammonium uptake. *Nature* **2007**, *446*, 195–198. [CrossRef] [PubMed]
13. Straub, T.; Ludewig, U.; Neuhäuser, B. The kinase CIPK23 inhibits ammonium transport in *Arabidopsis thaliana*. *Plant Cell* **2017**, *29*, 409–422. [CrossRef]
14. Gao, Y.X.; Li, Y.; Yang, X.X.; Li, H.J.; Shen, Q.R.; Guo, S.W. Ammonium nutrition increases water absorption in rice seedlings (*Oryza sativa* L.) under water stress. *Plant Soil* **2010**, *331*, 193–201. [CrossRef]
15. Ding, L.; Gao, C.; Li, Y.; Zhu, Y.; Xu, G.; Guo, S.W. The enhanced drought tolerance of rice plants under ammonium is related to aquaporin (AQP). *Plant Sci.* **2015**, *234*, 14–21. [CrossRef]
16. Kant, S.; Kant, P.; Lips, H.; Barak, S. Partial substitution of NO_3^- by NH_4^+ fertilization increases ammonium assimilating enzyme activities and reduces the deleterious effects of salinity on the growth of barley. *J. Plant Physiol.* **2007**, *164*, 303–311. [CrossRef] [PubMed]
17. Fernández-Crespo, E.; Camanes, G.; García-Agustín, P. Ammonium enhances resistance to salinity stress in citrus plants. *J. Plant Physiol.* **2012**, *169*, 1183–1191. [CrossRef] [PubMed]
18. Huang, L.L.; Li, M.J.; Shao, Y.; Sun, T.T.; Li, C.Y.; Ma, F.W. Ammonium uptake increases in response to PEG-induced drought stress in *Malus hupehensis* Rehd. *Environ. Exp. Bot.* **2018**, *151*, 32–42. [CrossRef]
19. Meng, S.; Zhang, C.X.; Su, L.; Li, Y.M.; Zhao, Z. Nitrogen uptake and metabolism of *Populus simonii* in response to PEG-induced drought stress. *Environ. Exp. Bot.* **2016**, *123*, 78–87. [CrossRef]
20. Bu, Y.; Takano, T.; Liu, S. The role of ammonium transporter (AMT) against salt stress in plants. *Plant Signaling Behav.* **2019**, *14*, 8. [CrossRef]
21. Shelden, M.C.; Dong, B.; de Bruxelles, G.L.; Trevaskis, B.; Whelan, J.; Ryan, P.R.; Howitt, S.M.; Udvardi, M.K. *Arabidopsis* ammonium transporters, *AtAMT1;1* and *AtAMT1;2*, have different biochemical properties and functional roles. *Plant Soil* **2001**, *231*, 151–160. [CrossRef]

22. Gu, R.; Duan, F.; An, X.; Zhang, F.; Von Wirén, N.; Yuan, L. Characterization of AMT-mediated high-affinity ammonium uptake in roots of maize (*Zea mays* L.). *Plant Cell Physiol.* **2013**, *54*, 1515–1524. [CrossRef]
23. Liu, R.H.; Meng, J.L. MapDraw: A Microsoft Excel macro for drawing genetic linkage maps based on given genetic linkage data. *Yi Chuan* **2003**, *25*, 317–321.
24. Chang, S.; Puryear, J.; Cairney, J. Simple and efficient method for isolating RNA from pine trees. *Plant Mol. Biol. Rep.* **1993**, *11*, 113–116. [CrossRef]
25. Sun, T.; Jia, D.; Huang, L.L.; Shao, Y.; Ma, F.W. Comprehensive genomic identification and expression analysis of the nucleobase-ascorbate transporter (NAT) gene family in apple. *Sci. Hortic.* **2016**, *198*, 473–481. [CrossRef]
26. Livak, K.J.; Schmittgen, T.D. Analysis of relative gene expression data using real-time quantitative PCR and the $2^{-\Delta\Delta CT}$ method. *Methods* **2001**, *25*, 402–408. [CrossRef]
27. Marini, A.M.; Soussi-Boudekou, S.; Vissers, S.; Andre, B. A family of ammonium transporters in *Saccharomyces cerevisiae*. *Mol. Cell Biol.* **1997**, *17*, 4282–4293. [CrossRef] [PubMed]
28. Yang, S.Y.; Hao, D.L.; Cong, Y.; Jin, M.; Su, Y.H. The rice OsAMT1;1 is a proton-independent feedback regulated ammonium transporter. *Plant Cell Rep.* **2015**, *34*, 321–330. [CrossRef] [PubMed]
29. Lanquar, V.; Loqué, D.; Hörmann, F.; Yuan, L.; Bohner, A.; Engelsberger, W.R.; Lalonde, S.; Schulze, W.X.; Von Wirén, N.; Frommer, W.B. Feedback inhibition of ammonium uptake by a phospho-dependent allosteric mechanism in Arabidopsis. *Plant Cell* **2009**, *21*, 3610–3622. [CrossRef] [PubMed]
30. Hao, D.L.; Zhou, J.Y.; Yang, S.Y.; Qi, W.; Yang, K.J.; Su, Y.H. Function and Regulation of Ammonium Transporters in Plants. *Int. J. Mol. Sci.* **2020**, *21*, 3557. [CrossRef] [PubMed]
31. Ninnemann, O.; Jauniaux, J.C.; Frommer, W.B. Identification of a high affinity NH_4^+ transporter from plants. *EMBO J.* **1994**, *13*, 3464–3471. [CrossRef]
32. Sonoda, Y.; Ikeda, A.; Saiki, S.; Yamaya, T.; Yamaguchi, J. Feedback regulation of the ammonium transporter gene family AMT1 by glutamine in rice. *Plant Cell Physiol.* **2003**, *44*, 1396–1402. [CrossRef]
33. Giehl, R.F.; Laginha, A.M.; Duan, F.; Rentsch, D.; Yuan, L.; Von Wirén, N. A Critical Role of AMT2;1 in Root-To-Shoot Translocation of Ammonium in *Arabidopsis*. *Mol. Plant* **2017**, *10*, 1449–1460. [CrossRef]
34. Von Wirén, N.; Lauter, F.R.; Ninnemann, O.; Gillissen, B.; Walch-Liu, P.; Engels, C.; Jost, W.H.; Frommer, W.B. Differential regulation of three functional ammonium transporter genes by nitrogen in root hairs and by light in leaves of tomato. *Plant J. Cell Mol. Biol.* **2000**, *21*, 167–175. [CrossRef]
35. Lee, Y.H.; Tegeder, M. Selective expression of a novel high-affinity transport system for acidic and neutral amino acids in the tapetum cells of *Arabidopsis* flowers. *Plant J.* **2004**, *40*, 60–74. [CrossRef]
36. Yuan, L.; Graff, L.; Loqué, D.; Kojima, S.; Tsuchiya, Y.N.; Takahashi, H.; Von Wirén, N. AtAMT1;4, a Pollen-Specific High-Affinity Ammonium Transporter of the Plasma Membrane in *Arabidopsis*. *Plant Cell Physiol.* **2009**, *50*, 13–25. [CrossRef]
37. D'Apuzzo, E.; Rogato, A.; Simon-Rosin, U.; Alaoui, H.E.; Barbulova, A.; Betti, M.; Dimou, M.; Katinakis, P.; Márquez, A.J.; Marini, A.; et al. Characterization of three functional high-affinity ammonium transporters in *Lotus japonicus* with differential transcriptional regulation and spatial expression. *Plant Physiol.* **2004**, *134*, 1763–1774. [CrossRef]
38. Ranathunge, K.; El-Kereamy, A.; Gidda, S.; Bi, Y.M.; Rothstein, S.J. *AMT1;1* transgenic rice plants with enhanced NH_4^+ permeability show superior growth and higher yield under optimal and suboptimal NH_4^+ conditions. *J. Exp. Bot.* **2014**, *65*, 965–979. [CrossRef]
39. Zhong, L.; Huang, X.; Zhu, Y.; Kou, E.; Liu, H.; Sun, G.; Chen, R.; Songm, S. Characterization and expression analysis of *BcAMT1;4*, an ammonium transporter gene in flowering Chinese cabbage. *Hortic. Environ. Biotechnol.* **2019**, *60*, 563–572. [CrossRef]
40. Gansel, X.; Munos, S.; Tillard, P.; Gojon, A. Differential regulation of the NO_3^- and NH_4^+ transporter genes *AtNrt2.1* and *AtAmt1.1* in Arabidopsis: Relation with long-distance and local controls by N status of the plant. *Plant J.* **2001**, *26*, 143–155. [CrossRef]
41. Li, H.; Han, J.; Chang, Y.; Lin, J.; Yang, Q. Gene characterization and transcription analysis of two new ammonium transporters in pear rootstock (*Pyrus betulaefolia*). *J. Plant Res.* **2016**, *129*, 737–748. [CrossRef]
42. Huang, L.L.; Li, M.J.; Zhou, K.; Sun, T.T.; Hu, L.Y.; Li, C.Y.; Ma, F.W. Uptake and metabolism of ammonium and nitrate in response to drought stress in *Malus prunifolia*. *Plant Physiol. Biochem.* **2018**, *127*, 185–193. [CrossRef] [PubMed]
43. Hessini, K.; Ben, H.K.; Gandour, M.; Mejri, M.; Abdelly, C.; Cruz, C. Ammonium nutrition in the halophyte *Spartina alterniflora* under salt stress, evidence for a priming effect of ammonium? *Plant Soil* **2013**, *370*, 163–173. [CrossRef]
44. Yuan, L.; Gu, R.; Xuan, Y.; Smith-Valle, E.; Loqué, D.; Frommer, W.B.; Von Wirén, N. Allosteric regulation of transport activity by heterotrimerization of *Arabidopsis* ammonium transporter complexes in vivo. *Plant Cell* **2013**, *25*, 974–984. [CrossRef]
45. Ludewig, U.; Neuhäuser, B.; Dynowski, M. Molecular mechanisms of ammonium transport and accumulation in plants. *FEBS Lett.* **2007**, *581*, 2301–2308. [CrossRef] [PubMed]